

High-Resolution Measurement and Analysis of the Infrared Spectrum of Nitric Acid near 1700 cm^{-1}

A. G. MAKI

Molecular Spectroscopy Division, National Bureau of Standards, Washington, D. C. 20234

AND

J. S. WELLS

Time and Frequency Division, National Bureau of Standards, Boulder, Colorado 80303

The infrared spectrum of the ν_2 band of nitric acid (HNO_3) has been measured with a tunable diode laser in the frequency interval from 1690 to 1727 cm^{-1} . A total of 430 assigned transitions have been analyzed to yield a set of nine rovibrational constants for the upper state with a standard deviation of 0.0012 cm^{-1} . The band is primarily *B* type with a band center at $1709.568 \pm 0.005\text{ cm}^{-1}$. Because of the absence of perturbations, the band constants can be used to calculate transition frequencies and relative intensities with a high degree of accuracy.

I. INTRODUCTION

Nitric acid (HNO_3) has been observed in the earth's atmosphere (1-3) and is believed to be an important link in the complex chain of chemical reactions governing the concentration of ozone in the upper atmosphere. Because of this, there is considerable interest in monitoring the concentration of nitric acid in the atmosphere. Most monitoring techniques make use of spectroscopic measurements. To better understand and interpret those measurements it is necessary to make modeling calculations based on known spectroscopic properties. Such calculations must simulate the atmospheric path under observation by taking into account the varying conditions of concentration, temperature, and pressure. The present work is the first high-resolution infrared study of the 1700-cm^{-1} band that yields a set of rovibrational constants that could be used in such modeling calculations.

Chevillard and Giraudet (4) have recently published the results of an analysis of the ν_5 and $2\nu_9$ infrared bands near 880 cm^{-1} . They were only able to determine the band centers and effective $\Delta\bar{B}$ and ΔC constants because they only resolved clumps of lines separated by about 0.4 cm^{-1} . While this paper was in preparation a more complete analysis of the ν_5 band, which was observed by Brockman *et al.* (5), was published by Dana (6).

The 1709-cm^{-1} ν_2 band has been observed with low resolution by several earlier workers (7, 8). Recently Farrow *et al.* (9) have studied the absorption vs

TABLE I
OCS Transitions Used to Calibrate the HNO₃ Spectrum

Spectral Region (cm ⁻¹)	OCS Calibration	
	Line	cm
1726.0 - 1726.2	R(42)	1726.0913
1725.5 - 1725.9	R(41)	1725.7921
1723.8 - 1724.4	R(36)	1724.2585
	R(35)	1723.9442
1723.2 - 1723.7	R(34)	1723.6274
	R(33)	1723.3081
1721.6 - 1723.2	R(32)	1722.9863
	R(31)	1722.6620
	R(30)	1722.3352
	R(29)	1722.0059
	R(28)	1721.6741
	R(27)	1721.3398
1720.3 - 1721.5	R(26)	1721.0030
	R(25)	1720.6638
	R(24)	1720.3220
	R(6)	1713.7479
1712.8 - 1713.8	R(5)	1713.3593
	R(4)	1712.9682
1707.8 - 1708.7	P(6)	1708.5054
	P(7)	1708.0851
1704.7 - 1706.0	P(12)	1705.9468
	P(13)	1705.5119
	P(14)	1705.0745
	P(16)	1704.1925
1702.9 - 1704.2	P(17)	1703.7478
	P(18)	1703.3007
	P(31)	1697.2672
	P(32)	1696.7861
	P(40)	1692.8495
	P(41)	1692.3465
1691.5 - 1691.8	P(42)	1691.8410
1690.7 - 1691.4	P(43)	1691.3331
	P(44)	1690.8228

pressure curves for the absorption of three different CO laser lines by HNO₃ near 1700 cm⁻¹. Their results were interpreted in terms of pressure-broadening coefficients and other parameters for nitric acid. An NBS-NOAA team (10) has used the diode laser spectrum of this same band of nitric acid in a measurement of the rate constant for nitric acid plus nitric oxide. The present analysis shows what transitions are involved in both of these measurements.

The microwave spectrum of nitric acid has been studied by Millen and Morten (11, 12) and then by Cox and Riveros (13), who measured some of the rarer isotopic species. Most recently Cazzoli and DeLucia (14) have measured many new high-frequency rotational transitions. These microwave studies have provided excellent rotational constants for the ground state of nitric acid and we have used the microwave data in our analysis.

II. EXPERIMENTAL DETAILS

The spectrum of HNO₃ was recorded using the diode laser spectrometer described earlier by Todd and Olson (15). Calibration was provided by absorption lines of carbonyl sulfide (OCS) (16). The calibration frequencies were determined by measuring OCS on the NBS 2.35-m Littrow grating spectrometer and combining those measurements with precisely measured rotational constants for OCS (see Ref. (17)). The estimated absolute uncertainty of the measurements (about ±0.005 cm⁻¹) is only slightly inferior to the absolute uncertainty in the OCS calibration. The calibration frequencies used in this work are given in Table

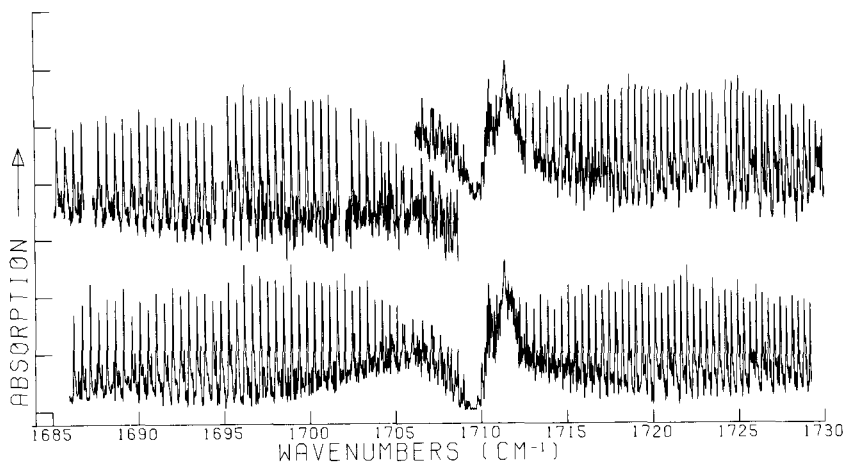


FIG. 1. The strongest portion of the ν_2 band of HNO₃. The lower trace is a theoretical spectrum produced by the constants given in Table II. The upper traces give the grating spectrum taken with a slit width of 0.035 cm⁻¹, a pathlength of 61 cm, and a pressure of about 1 Torr. Note that the two upper traces are slightly displaced from each other. The small gaps in the upper traces were caused by interruptions required to obtain the frequency calibration.

I, which also indicates the wavenumber intervals for which we obtained laser diode measurements of HNO₃.

Interpolation between calibration lines was provided by the fringe pattern generated by either of two solid germanium etalons, one 2.5 cm long and one 7.5 cm long, yielding fringes spaced by 0.049 and 0.016 cm⁻¹, respectively. By means of a beam splitter, two detectors, and a dual pen recorder the fringe pattern was recorded simultaneously with the HNO₃ spectrum. Each spectral measurement also contained at least one calibration line added to the HNO₃ spectrum by substituting absorption cells at the appropriate moment for recording the calibration line. Each spectral trace required less than 3 min to record and the etalon had a special housing to reduce the possibility of thermal drift.

During the measurements the HNO₃ sample was held in a 40-cm-long glass absorption cell with CaF₂ windows. All of the measurements were made with less than 1 Torr (<133 Pa) HNO₃.

III. DETAILS OF THE APPEARANCE AND ASSIGNMENTS OF THE BAND

According to the assignment of McGraw *et al.* (7) and of others, the 1709-cm⁻¹ band must be the ν_2 N-O asymmetric stretching band. Since the vibrational motion is entirely within the plane of the molecule, and since the molecule is planar and has C_s symmetry, the band under study must be a hybrid A -type and B -type band.

The upper curve of Fig. 1 shows a grating spectrometer scan of the strongest portion of the ν_2 band. Below the experimental spectrum we have plotted a spectrum calculated using the constants resulting from this work. In Fig. 2 we show a high-resolution diode laser spectrum between 1721 and 1723 cm⁻¹.

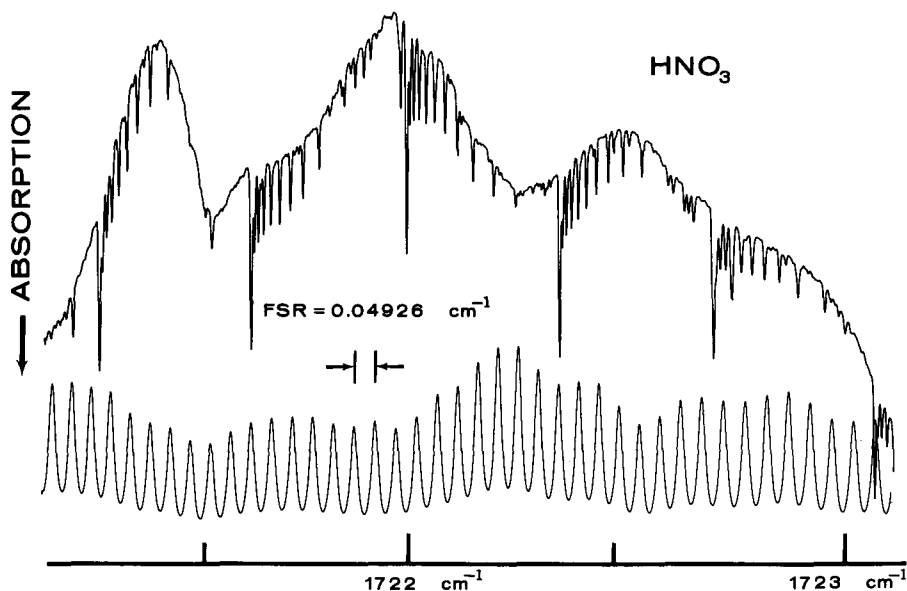


FIG. 2. Diode laser spectrum of a portion of the ν_2 band of HNO_3 (pathlength, 40 cm; pressure, <1 Torr). The lower curve is the fringe pattern produced by the etalon.

The low-resolution spectrum shows that the band is mostly a B -type band since it does not have a prominent, strong central Q -branch-like feature. Our calculated spectrum verifies the virtual absence of an A component to the dipole derivative (the principal difference being in the Q -branch region). We estimate that the A -type transitions must be at least 10 times weaker than the B -type transitions. For a B -type band the only allowed transitions must be of the types

$$ee \leftrightarrow oo \quad \text{and} \quad oe \leftrightarrow eo,$$

and the strongest transitions will be $\Delta J = 0, \pm 1$; $\Delta K_a = \pm 1$; $\Delta K_c = \pm 1$.

As can be seen in Fig. 1, the ν_2 band shows prominent P - and R -branch features separated by 0.4 cm^{-1} . Under high resolution each feature is found to be a clump of many closely spaced lines that converge to a strong feature (at the low-wavenumber end of the clump) that is obviously several unresolved lines. For an oblate planar molecule it is easy to show that each clump must consist of transitions coming from levels with quantum numbers that follow the series: $J'' = N$, $K_a'' = 0$ or 1 , $K_c'' = N$; $J'' = N - 1$, $K_a'' = 1$ or 2 , $K_c'' = N - 2$; $J'' = N - 2$, $K_a'' = 2$ or 3 , $K_c'' = N - 4$; etc., where the strongest transition will have $J'' = K_c''$ and the intensity will diminish as $J'' - K_c''$ increases. Each line is a doublet (with two possible values of K_a'') with a negligible splitting until K_c'' reaches a low value (about 10) at which point the asymmetry takes over and suddenly the splitting becomes very large and the series of lines in each clump appears to terminate. The point at which the asymmetry splitting becomes significant is easily calculated from the well-known ground-state constants and a first estimate of the upper-state constants. The onset of the asymmetry splitting provided an important clue

to the correct assignment and especially to the number of unresolved lines present in the initial strong line of each clump.

In our diode spectra and in a preliminary theoretical spectrum that was calculated we noticed a prominent series of sharp lines with a spacing of $2\bar{B}$ (0.8 cm⁻¹). This series turned out to be due to the *P*- and *R*-branch transitions of the unresolved doublet from states given by $J'' = K''_a$ and $K''_c = 0$ or 1. This series of strong lines was another valuable aid in making the assignments as it determined which of the above-mentioned clumps (with 0.4-cm⁻¹ spacing) involved even values of K''_c and which involved odd values.

Finally, in the *Q*-branch region the spectrum is dominated by many overlapping series of *Q*-branch lines with roughly equal spacing of about 0.05 cm⁻¹. Each series is described by a single value of K''_c and begins with a weak line for which either $J'' = K''_a$ or $J' = K''_a$. The lines go through an intensity maximum for $J - K_a \approx 10$ and then fade out slowly.

The *Q*-branch lines could only be assigned after the *P*- and *R*-branch transitions had been assigned and fit. It was then possible to use the derived band constants to predict the *Q*-branch transitions and intensities with confidence. The assignments for all but the highest quantum numbers followed immediately from the predicted spectrum and a bootstrap procedure starting with the low quantum numbers soon led to the assignment of the higher-quantum-number *Q*-branch transitions.

IV. THE ROVIBRATIONAL CONSTANTS

The assigned transitions were fit to a set of upper-state constants using the nonlinear least-squares program developed by one of the authors (A.M.) for fitting asymmetric rotor spectra. This program fits the transition frequencies to the *prolate* rotor constants defined by the Hamiltonian

$$\begin{aligned} \mathcal{H} = & (1/2)(\mathcal{B} + \mathcal{C})P^2 + (\mathcal{A} - (1/2)(\mathcal{B} + \mathcal{C}))[P_z^2 - b_p P_-^2] - \Delta_J P^4 - \Delta_{JK} P_z^2 P^2 \\ & - \Delta_K P_z^4 - 2\delta_J P^2 P_-^2 - \delta_K [P_z^2 P_-^2 + P_-^2 P_z^2] + H_J P^6 + H_{JK} P^4 P_z^2 \\ & + H_{KJ} P^2 P_z^4 + H_K P_z^6 + 2h_J P^4 P_-^2 + h_{JK} P^2 [P_z^2 P_-^2 + P_-^2 P_z^2] \\ & + h_K [P_z^4 P_-^2 + P_-^2 P_z^4] - L_K P_z^8, \quad (1) \end{aligned}$$

where

$$P^2 = P_x^2 + P_y^2 + P_z^2,$$

$$P_-^2 = P_x^2 - P_y^2,$$

and b_p is the Wang asymmetry parameter. Although HNO₃ is an oblate rotor with the asymmetry parameter $\kappa = 0.73$, the asymmetric rotor program written in terms of prolate matrix elements presented no difficulty in rapidly converging to the correct solution.

The most undesirable consequence of using the prolate rotor constants was apparently the very high correlation that exists between h_{JK} and the other sextic constants for the data base at hand. When h_{JK} was included as a variable in the least-squares analysis, most of the sextic terms were no larger than twice their standard deviation and the correlation coefficients indicated a very high degree of correlation

TABLE II
Prolate Rovibrational Constants for HNO₃ Based on Eq. (1)

Ground State Constants		Changes in the Constants for the ν_0 Band	
G	0.4339970(22) ^a	G'-G''	-2.2785(89)×10 ⁻³
B	0.40360987(20)	B'-B''	-0.7794(65)×10 ⁻³
C	0.20883222(20)	C'-C''	-0.69687(178)×10 ⁻³
Δ_J	0.295120(1200)×10 ⁻⁶	$\Delta_J'-\Delta_J''$	0.850(833)×10 ⁻⁸
Δ_{JK}	-0.152151(684)×10 ⁻⁶	$\Delta_{JK}'-\Delta_{JK}''$	-4.62(400)×10 ⁻⁸
Δ_K	0.246816(445)×10 ⁻⁶	$\Delta_K'-\Delta_K''$	3.51(410)×10 ⁻⁸
ϵ_J	0.126225(106)×10 ⁻⁶	$\epsilon_J'-\epsilon_J''$	0.395(415)×10 ⁻⁸
ϵ_K	0.249683(286)×10 ⁻⁶	$\epsilon_K'-\epsilon_K''$	-0.504(1160)×10 ⁻⁸
H _J	-3.138(1848)×10 ⁻¹²	H _{J}'-H_{J}''}}	[0.0] ^b
H _{JK}	0.977(80)×10 ⁻¹²	H _{JK}'-H_{JK}''}}	[0.0]
H _{KJ}	-4.333(561)×10 ⁻¹²	H _{KJ}'-H_{KJ}''}}	[0.0]
H _K	4.549(468)×10 ⁻¹²	H _{K}'-H_{K}''}}	[0.0]
h _J	-0.031(34)×10 ⁻¹²	h _{J}'-h_{J}''}}	[0.0]
h _{JK}	[0.0] ^b	h _{JK}'-h_{JK}''}}	[0.0]
h _K	1.075(128)×10 ⁻¹²	h _{K}'-h_{K}''}}	[0.0]

$\nu_0 = 1709.5676(4)^c$

- a) The uncertainty (twice the estimated standard deviation) in the last digits is given in parentheses.
 b) Fixed values are indicated by square brackets.
 c) Because of uncertainties in the absolute calibration, the band center (ν_0) has an additional uncertainty of ± 0.005 cm⁻¹ (see text).

Note. All constants in cm⁻¹.

among all the sextic terms. Since the value of h_{JK} was about five times smaller than its standard deviation, it was eliminated from the fit. Removing the h_{JK} term reduced much of the correlation among the sextic terms although H_K , H_{KJ} , and h_K still show a high, but not alarming, degree of correlation.

Since our fitting program used a prolate Hamiltonian and was unable to handle the oblate rotor constants given by Cazzoli and DeLucia (14), we used their microwave data (kindly given to us in advance of publication) to determine a set of prolate ground-state constants. We had to omit the $J'' = 50$, $K''_a = 46$ line due to a storage limitation on the size of our prolate energy matrix. In addition to the microwave data of Cazzoli and DeLucia (14) we also used the measurements published by Millen and Morton (11, 12). The 136 microwave transitions were combined with 76 infrared ground-state combination differences resulting from our diode laser measurements. The resulting prolate rotor ground-state constants given in Table II were then used to calculate ground-state energy levels which, when combined with the infrared transitions, allowed us to determine the upper-state energy levels and fit them to a set of upper-state constants.

A total of 430 infrared transitions were used in the determination of the upper-state constants. The standard deviation of the fit with all lines given unit weight was 0.0012 cm⁻¹. The transitions covered low and intermediate values of J ranging from 8 to 40; and the K_a and K_c quantum numbers included the complete range from 0 to 40. The band was remarkably free of any evidence of perturbations. Although

perturbations from distant levels can not be ruled out completely, the small change from the ground-state values (for all the rotational constants and especially for the centrifugal distortion constants) leads us to believe that this band is as free from perturbations as it is possible to be.

Table II gives the differences in the rotational constants between the upper and lower states of the ν_2 band since such differences are relatively insensitive (i.e., uncorrelated) to the values of the lower-state constants used in the analysis. We believe that the constants given in Table II can be used to reliably calculate all the strong transitions from the ground state of HNO₃ in the range from 1690 to 1727 cm⁻¹. We have used those constants to construct an atlas of transition frequencies and intensities for this band in the above frequency range. The atlas has been deposited at the editorial office and it is also available from one of the authors (A.M.). The constants were also used to calculate the theoretical low-resolution spectrum shown as the lower curve in Fig. 1. This theoretical spectrum only included transitions up to $J'' = 50$ and $K''_a = 48$ where the lines still have significant intensity. Nevertheless, the theoretical spectrum comes surprisingly close to duplicating the observed spectrum.

In constructing such a theoretical absorption spectrum one must remember that it only represents those transitions that occur through the absorption by molecules in the ground vibrational state. In HNO₃ at room temperature only 78% of the molecules will be in the ground state. In addition, 8.4% of the molecules will be in the lowest vibrational state (at 293 K) and the remaining 13% will be in higher vibrational states. Because of this vibrational partitioning, about 22% of the total absorption of the 1709-cm⁻¹ band will not be included in the theoretical spectrum. Most of the missing absorption intensity will be evenly distributed in weak transitions throughout the band. We have noticed many weak features in our spectrum that do not correspond to any calculated ground-state transitions and believe that they are transitions from excited vibrational states (hot-band transitions). When such hot-band transitions overlap ground-state transitions, the ground-state transitions may appear anomalously strong. Aside from such hot-band effects, which will be reduced as the temperature is lowered, the theoretical spectrum gives a close approximation to the observed spectrum for both the positions and relative intensities of the lines.

ACKNOWLEDGMENTS

The authors thank G. Cazzoli and F. C. DeLucia for sending their microwave measurements prior to publication. The authors would also like to acknowledge the assistance of Wm. Bruce Olson and Terry R. Todd, who did most of the work of designing and assembling the diode spectrometer used in this work. They also wish to thank Robert L. Sams, who measured the grating spectrum. We acknowledge contributions by G. E. Streit (former NOAA Boulder, Colorado, Postdoctoral Fellow) and partial support by the NBS Office of Air and Water Measurements during some preliminary phases of the work. We express our gratitude to the NASA Upper Atmospheric Research Office for their current partial support of this research.

Note added in proof. The value of h_k given in Table II should be multiplied by two to give $h_k = 2.150(256) \times 10^{-12}$ cm⁻¹.

RECEIVED: July 23, 1979

REFERENCES

1. D. G. MURCRAY, T. G. KYLE, F. H. MURCRAY, AND W. J. WILLIAMS, *Nature (London)* **218**, 78-79 (1968).
2. J. C. FONTANELLA, A. GIRARD, L. GRAMONT, AND N. LOUISNARD, *Appl. Opt.* **14**, 825-839 (1975).
3. C. M. BRADFORD, F. H. MURCRAY, J. W. VANALLEN, J. N. BROOKS, D. G. MURCRAY, AND A. GOLDMAN, *Geophys. Res. Lett.* **3**, 387-390 (1976).
4. J. P. CHEVILLARD AND R. GIRAUDET, *J. Phys. (Paris)* **39**, 517-520 (1978).
5. P. BROCKMAN, C. H. BAIR, AND F. ALLARIO, *Appl. Opt.* **17**, 91-100 (1978).
6. V. DANA, *Spectrochim. Acta Part A* **34**, 1027-1031 (1978).
7. G. E. MCGRAW, D. L. BERNITT, AND I. C. HISATSUNE, *J. Chem. Phys.* **42**, 237-244 (1965).
8. A. GOLDMAN, T. G. KYLE, AND F. S. BONOMO, *Appl. Opt.* **10**, 65-73 (1971).
9. L. A. FARROW, R. E. RIGHTON, AND C. P. KARNAS, *Appl. Opt.* **18**, 76-81 (1979).
10. G. E. STREIT, J. S. WELLS, CARLETON J. HOWARD, AND F. C. FEHSENFELD, *J. Chem. Phys.* **70**, 3439-3443 (1979).
11. D. J. MILLEN AND J. R. MORTON, *Chem. Ind.*, 954 (1956).
12. D. J. MILLEN AND J. R. MORTON, *J. Chem. Soc.*, 1523-1528 (1960).
13. A. P. COX AND J. M. RIVEROS, *J. Chem. Phys.* **42**, 3106-3112 (1965).
14. G. CAZZOLI AND F. C. DELUCIA, *J. Mol. Spectrosc.* **76**, 131-141 (1979).
15. T. R. TODD AND W. B. OLSON, *J. Mol. Spectrosc.* **74**, 190-202 (1979).
16. A. G. MAKI, W. B. OLSON, AND R. L. SAMS, *J. Mol. Spectrosc.* **81**, 122-138 (1980).
17. A. G. MAKI, *J. Phys. Chem. Ref. Data* **3**, 221-224 (1974).